EUROPEAN OPEN SCIENCE SPACE

COLLECTION OF SCIENTIFIC PAPERS

9th International Scientific and Practical Conference

NEW HORIZONS IN SCIENTIFIC RESEARCH: CHALLENGES AND SOLUTIONS

ISSUE №115

eoss-conf.com

November 23-25, 2026
Marseille, France

EUROPEAN OPEN SCIENCE SPACE

Proceedings of the 9th International Scientific and Practical Conference

"New Horizons in Scientific Research: Challenges and Solutions"

November 23-25, 2026

Marseille, France

Collection of Scientific Papers

France, 2026

UDC 01.1

Collection of Scientific Papers with the Proceedings of the 9th International Scientific and Practical Conference «New Horizons in Scientific Research: Challenges and Solutions» (November 23-25, 2026, Marseille, France). European Open Science Space. 2026.

ISBN 979-8-89704-962-2 (series)
DOI 10.70286/EOSS-23.11.2026



The conference is included in the Academic Research Index ReserchBib International catalog of scientific conferences.



The conference is registered in the database of scientific and technical events of UkrISTEI to be held on the territory of Ukraine (Certificate №569 dated 28.07.2026).



The materials of the conference are publicly available under the terms of the CC BY-NC 4.0 International license.

The materials of the collection are presented in the author's edition and printed in the original language. The authors of the published materials bear full responsibility for the authenticity of the given facts, proper names, geographical names, quotations, economic and statistical data, industry terminology, and other information.

ISBN 979-8-89704-962-2

EUROPEAN OPEN SCIENCE SPACE

© Participants of the conference, 2026
© Collection of scientific papers, 2026
© European Open Science Space, 2026

Section: Technical Sciences

Кімстач О., Олейніченко В.О.
ДИФЕРЕНЦІАЛЬНІ ЗАХИСТИ НА ОСНОВІ СТРУМУ ТА НАПРУГИ ДЛЯ ТРАНСФОРМАТОРУ ІНВЕРТОРУ……. 800

Яценко І., Степаненко М.
ЗАСТОСУВАННЯ НЕЧІТКОЇ ЛОГІКИ ДЛЯ КОМПЛЕКСНОГО ДІАГНОСТУВАННЯ СИЛОВИХ ТРАНСФОРМАТОРІВ…….. 802

Мельник Р., Мельник О.
ГЕОІНФОРМАЦІЙНЕ МОДЕЛЮВАННЯ ТА ТРИВИМІРНА ВІЗУАЛІЗАЦІЯ МАРШРУТІВ МОНІТОРИНГУ НАДЗВИЧАЙНИХ СИТУАЦІЙ ІЗ ЗАСТОСУВАННЯМ БЕЗПІЛОТНИХ ЛІТАЛЬНИХ АПАРАТІВ…… 805

Пугач І., Харченко В., Пугач І.
ЗНАЧЕННЯ ОБІЗНАНОСТІ ПІД ЧАС ДОСЛІДЖЕННЯ ОБОВ'ЯЗКІВ КОНТРОЛЮ ТА РЕАГУВАННЯ У СУДОВІЙ ІНЖЕНЕРНО-ТЕХНІЧНІЙ ЕКСПЕРТИЗІ……..... 809

Горлов О., Воронько І., Миронова С., Бєсєдіна О.
ВИМОГИ, ЩО ЗУМОВЛЮЮТЬ ПОЗИТИВНУ ОЦІНКУ ТЕХНОЛОГІЧНОСТІ ЗВАРНИХ КОНСТРУКЦІЙ……. 815

Babanova O., Shevchenko A., Prasol S.
ANALYSIS OF MODERN EQUIPMENT AND METHODS FOR THE COMMINUTION AND CLASSIFICATION OF BULK FOOD PRODUCTS 820

Khvostivskyi M., Iliushenko I., Khvostivskyi O.
AUTOMATED ASSESSMENT OF POST-STRESS RECOVERY USING PULSE SIGNAL PARAMETERS……. 826

Murahovska O.
DEVELOPMENT OF PARTIAL EFFICIENCY CRITERIA FOR SEARCHING FOR GROUP OBJECTS USING AN UNMANNED AERIAL VEHICLE…… 831

Section: Tourism and Hotel and Restaurant Business

Куцик Л.
РОЗРОБЛЕННЯ СУХИХ ХАРЧОВИХ СУМІШЕЙ ДЛЯ ШВИДКОГО ПРИГОТУВАННЯ ОМЛЕТУ В ПОЛЬОВИХ УМОВАХ ХАРЧУВАННЯ ВІЙСЬКОВОСЛУЖБОВЦІВ ТА ТУРИСТІВ…… 835

3. Gupta, A., & Yan, D. S. (2016). Mineral processing design and operations: An introduction (2nd ed.). Amsterdam: Elsevier. 882 p. URL : https://doi.org/10.1016/C2014-0-01236-1.
4. Daniel, M. J., & Morrell, S. (2004). HPGR model verification and scale-up. Minerals Engineering, 17(11–12). Pp. 1149–1161. URL : https://doi.org/10.1016/j.mineng.2004.05.016.
5. Shapiro, M., & Galperin, V. (2005). Air classification of solid particles: A review. Chemical Engineering and Processing, 44(2). Pp. 279–285. URL : https://doi.org/10.1016/j.cep.2004.02.022.
6. Nayak, D. K., Das, D. P., Behera, S. K., & Das, S. P. (2020). Monitoring the fill level of a ball mill using vibration sensing and artificial neural network. Neural Computing and Applications, 32. Pp. 1501–1511. URL : https://doi.org/10.1007/s00521-019-04555-5.

AUTOMATED ASSESSMENT OF POST-STRESS RECOVERY USING PULSE SIGNAL PARAMETERS

Khvostivskyi Mykola
Ph.D., Associate Professor
Iliushenko Ivan
Student
Khvostivskyi Oleksandr
Student
Ternopil Ivan Puluj National Technical University, Ukraine

Problem statement. High-risk work requires decisions under time pressure and emotional strain. Task completion time and errors describe performance during exposure, whereas physiological recovery provides information about the persistence of the response after the task has ended. Quantifying this recovery requires an explicit rule for identifying a sustained return to an individual resting state.

Reflectance photoplethysmography provides a non-invasive pulse recording that covers rest, exposure, and recovery [1]. A Stroop task was associated with increased pulse rate, decreased amplitude, and changes in variability [2]. Non-contact optical measurements were used to study peripheral hemodynamics under cognitive and psychological stressors [3]. Stress-related parameter changes were also incorporated into a pulse signal simulation model [4].

Aim. The study developed a method and a MATLAB application for determining recovery duration from pulse-cycle amplitude and duration. The resulting physiological measure was considered alongside task performance in assessing candidates' psychoemotional readiness for high-risk work. The investigation comprised signal modeling [9], joint parameter analysis, verification, and application testing. Fig. 1 shows the screen used to present the audiovisual task.



Fig. 1. Participant screen for the audiovisual fire evacuation task

Signal model and processing method. The recorded signal was represented as a sequence of pulse cycles with a slowly varying baseline and an additive disturbance [8]. Within the k-th cycle, its pulse component was expressed as

$$x(t) = b(t) + A_k \psi_k \left(\frac{t - t_k}{T_k}\right) + \varepsilon(t), \; t_k \leq t < t_k + T_k. \quad (1)$$

Here b(t) is the baseline, A_k is cycle amplitude, T_k is cycle duration, t_k is cycle onset, and ε(t) is an additive disturbance. The normalized waveform ψ_k combined forward and reflected components. Piecewise functions described the amplitude and duration trends across rest, exposure, and recovery, with random variations between adjacent cycles. A two-component representation of the pulse waveform was also used by Q. Tang et al. [5].

Complete cycles were delimited by successive minima, with the main maximum located inside each cycle [7]. Amplitude was measured relative to a local straight baseline joining the two minima. Median amplitude and duration were then obtained from valid complete cycles in each sliding window. Their joint deviation was calculated as

$$D_j^2 = (z_j - \hat{\mu}_0)^T S_0^{-1} (z_j - \hat{\mu}_0), \; z_j = (\tilde{A}, T)^T. \quad (2)$$

The vector $\hat{\mu}_0$ and covariance matrix S_0 were estimated from non-overlapping windows of initial rest. Accounting for covariance combined amplitude and duration without treating their resting fluctuations as independent.

For p=2 features and n>p resting windows, the prediction threshold was calculated using the F-distribution

$$h_\alpha = \frac{p(n-1)(n+1)}{n(n-p)} F_{p,n-p}^{-1}(1 - \alpha). \quad (3)$$

The normalized indicator was $J_j = D_j^2 / h\alpha$. After a response to the load had been detected, recovery was sought in windows lying entirely after exposure. A candidate return was confirmed when all valid windows remained at $J_j \leq 1$ for the prescribed confirmation interval. A threshold exceedance or a gap in valid data reset confirmation.

Window times were assigned to their right boundaries. Recovery duration was calculated from the end of exposure to the first qualifying window of the confirmed sequence. The confirmation time was recorded separately. The nominal α refers to a new resting window under the statistical assumptions of the prediction model.

Verification on a simulated signal. A control realization was generated and processed directly in MATLAB. Sampling frequency was 500 Hz and recording duration was 180 s. Exposure occupied 30-60 s, and the prescribed completion of recovery was 96 s. Processing used 5 s windows, a 0.5 s step, and an 8 s confirmation interval.

The analysis identified 227 complete cycles. Six non-overlapping resting windows and α=0.05 yielded h=20.254. Figure 2 reproduces the signal and processing results from the qualification work.

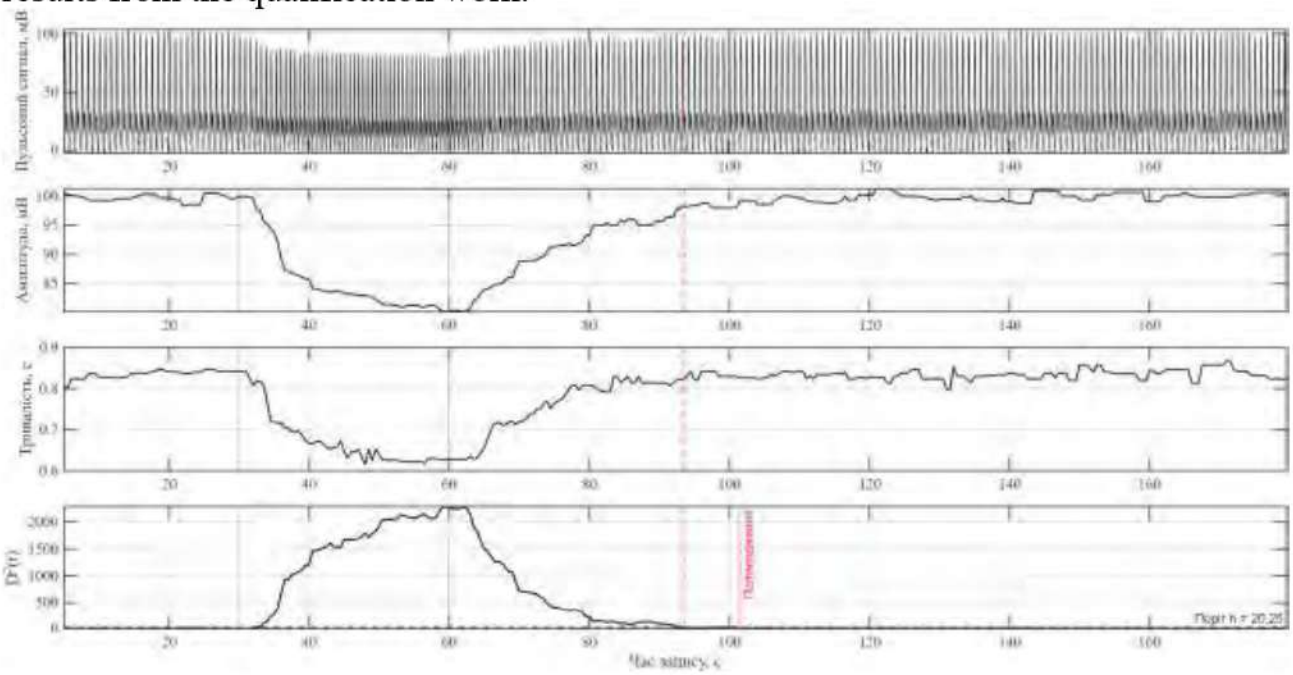

Fig. 2. Simulated pulse signal, cycle parameters, and joint deviation indicator

Return was estimated at 93.5 s and confirmed at 101.5 s. The reference recovery duration was 36.0 s, whereas the estimate was 33.5 s. Thus, the estimate preceded the specified model endpoint by 2.5 s. The relative error was

$$\delta = |33.5 - 36.0| / 36.0 \times 100\% = 6.94\% \approx 6.9\%. \quad (4)$$

This error characterizes the control realization. The threshold defined statistical compatibility with initial rest, whereas the model reference marked the end of the prescribed systematic trend. The 8 s confirmation interval was an additional observation period and was recorded separately from recovery duration.

Software implementation and testing. The application was implemented in MATLAB using App Designer interface components. Its tabs supported signal analysis, acquisition settings and stimulus control, test conditions, and results with an event log. File loading and serial-port settings were provided as separate ways of working with pulse data.

An audiovisual task presented a simulated fire evacuation scene with alternative actions and a response countdown. The operator could test the sound, preview the scenario, document conditions, and stop the session. The screenshot in Fig. 3 shows analysis of a signal loaded after recording.



Fig. 3. Application output for the previously recorded pulse signal

The loaded record was processed using 5 s windows, a 0.5 s step, and an 8 s confirmation interval. The six initial resting windows yielded $h=20.2541$ at $\alpha=0.05$. During exposure, median amplitude decreased approximately from 100 to 80 mV, and cycle duration decreased from about 0.83 to 0.61 s.

Following the end of exposure at 60 s, return to the resting region was estimated at 101.5 s and confirmed at 109.5 s. The recovery duration was therefore 41.5 s. These values relate to the loaded record and are distinct from the simulated verification results.

Interpretation of results. Table 1 separates the reference-based verification from application testing. This distinction is necessary because the simulated realization had a prescribed recovery endpoint, while an independent reference endpoint was not established for the loaded recording.

Table 1. Verification and application testing results

Indicator	Simulation	Loaded recording
Sampling frequency	500 Hz	500 Hz
Recording duration	180 s	180 s
Estimated return	93.5 s	101.5 s
Estimated recovery duration	33.5 s	41.5 s
Confirmation time	101.5 s	109.5 s
Relative recovery-duration error	6.9%	Reference unavailable

Conclusions. Joint processing of pulse-cycle amplitude and duration provided an individual recovery estimate relative to initial rest. Verification yielded a relative error of 6.9% for the simulated realization. Testing the MATLAB application with the loaded record yielded a recovery duration of 41.5 s and demonstrated graphical presentation of the underlying parameters and decision indicator.

The results support the technical feasibility of the procedure. Effects of mental stress and day-to-day variability on the reliability of pulse waveform assessment were examined in [6]. Establishing the relationship between recovery duration and readiness for a specific high-risk task requires independent task-performance measures and repeated recordings.

References

1. Allen J. Photoplethysmography and its application in clinical physiological measurement. Physiological Measurement. 2007. Vol. 28, no. 3. P. R1-R39. DOI: 10.1088/0967-3334/28/3/R01.
2. Minakuchi E. et al. Evaluation of mental stress by physiological indices derived from finger plethysmography. Journal of Physiological Anthropology. 2013. Vol. 32. Article 17. DOI: 10.1186/1880-6805-32-17.
3. McDuff D. et al. Non-contact imaging of peripheral hemodynamics during cognitive and psychological stressors. Scientific Reports. 2020. Vol. 10. Article 10884. DOI: 10.1038/s41598-020-67647-6.
4. Yavorska E., Strembitska O., Strembitskyi M., Pankiv I. Development of a simulation model of a photoplethysmographic signal under psychoemotional stress. Eastern-European Journal of Enterprise Technologies. 2021. Vol. 2, no. 9 (110). P. 36–45. DOI: 10.15587/1729-4061.2021.227001.
5. Tang Q., Chen Z., Ward R., Elgendi M. Synthetic photoplethysmogram generation using two Gaussian functions. Scientific Reports. 2020. Vol. 10. Article 13883. DOI: 10.1038/s41598-020-69076-x.
6. Fukuie M., Tarumi T., Yamabe T., Sugawara J. Reliability of Finger Photoplethysmogram Assessment: Effect of Mental Stress and Day-to-Day Variability. Artery Research. 2021. Vol. 27, no. 3. P. 107–111. DOI: 10.2991/artres.k.210208.001.
7. Hvostivska L.V., Osukhivska H.M., Hvostivskyy M.O., Shadrina H.M., Dediv I.Yu. Development of methods and algorithms for a stochastic biomedical signal period calculation in medical computer diagnostic systems [Розвиток методів та алгоритмів обчислення періоду стохастичних біомедичних сигналів для медичних комп'ютерно-діагностичних систем]. Visnyk NTUU KPI Seriia - Radiotekhnika Radioaparatobuduvannia, (79), pp. 78-84. doi: 10.20535/RADAP.2019.79.78-84.
8. Palaniza Y.B., Shadrina H.M., Khvostivskiy M.O., Dediv L.Ye., Dozorska O.F. Main theoretical basis of biosignals modeling. Znanstvena misel. Slovenia. 2018. №16. P. 39-44. ISSN 3124-1123.
9. Khvostivskiy M. O. Математична модель макромеханізму формування електроретиносигналу для підвищення достовірності офтальмодіагностичних систем [Mathematical model of the macromechanism of electroretinosignal formation to improve the reliability of ophthalmodiagnostic systems]: extended abstract of PhD dissertation (Tech. Sci.): 01.05.02. Ternopil, 2010. 20 p. (in Ukrainian). URL: https://elartu.tntu.edu.ua/handle/123456789/539.